Steam and Oxyhydrogen Addition Influence on Energy Usage by Range Extender—Battery Electric Vehicles

Andrzej Łebkowski

Department of Ship Automation, Gdynia Maritime University, Poland Morska St. 83, 81-225 Gdynia, Poland; a.lebkowski@we.am.gdynia.pl

check for updates

Abstract: The objective of this paper is to illustrate the benefits of the influence of the steam and oxyhydrogen gas (HHO) on the composition of emitted exhaust gases and energy usage of operating the internal combustion engine (ICE) that drives a generator-powered battery electric vehicle (BEV). The employed internal combustion generating sets can be used as trailer mounted electric energy sources allowing one to increase the range of BEV vehicles, mainly during long distance travel between cities. The basic configurations of hybrid and electric propulsion systems used in a given Electric Vehicles (xEV) includes all types of Hybrid Electric Vehicles (xHEV) and Battery Electric Vehicles (xBEV), which are discussed. Using the data collected during traction tests in real road traffic (an electric car with a trailer range extender (RE) fitted with ICE generators (5 kW petrol, 6.5 kW diesel), a mathematical model was developed in the Modelica package. The elaborated mathematical model takes into account the dynamic loads acting on the set of vehicles in motion and the electric drive system assisted by the work of RE. Conducted tests with steam and HHO additives for ICE have shown reduced (5–10%) fuel consumption and emissions (3–19%) of harmful gases into the atmosphere.

Keywords: electric vehicles; range extender; battery electric vehicle; hybrid electric vehicle

1. Introduction

Recent rapid intensification of climate change has motivated governments to discuss the possibility of introducing renewable energy sources in the transport sector. One of the theories claims that greenhouse gases emitted largely by transport are responsible for global warming and smog in cities [1]. On this basis, far-reaching steps have been taken to limit the emission of toxic substances by vehicles used in road transport [2]. These activities are aimed at the development of vehicles powered by electricity. However, the limitations of electric energy storage systems cause such vehicles have a relatively short range and the charging time is rather long—it typically ranges from several minutes to hours. To address these disadvantages, several different approaches were proposed to use various types of technological solutions, such as assembly of overhead traction lines supplying vehicles over the road on which they are moving [3] or construction of roads with a layer of photovoltaic panels with devices for wirelessly transferring energy directly to the vehicles [4]. Other proposals involve the use of electric drive systems [5–10] supported by an internal combustion engine (ICE) (a hybrid electric vehicle or HEV) [11], fuel cells (fuel cell electric vehicles or FCEVs) [12,13], supercapacitors [14], hydraulic [15] or pneumatic systems, as well as various types of electric batteries [16] with the possibility of charging them (plug-in hybrid electric vehicles or PHEVs) (Figure 1). The purpose of these technologies is to increase the range of vehicles while simultaneously minimizing greenhouse gas emissions. The impact analysis of using hybrid electric-combustion drive systems on the pollutants emitted by the vehicle has been presented in [17–19].
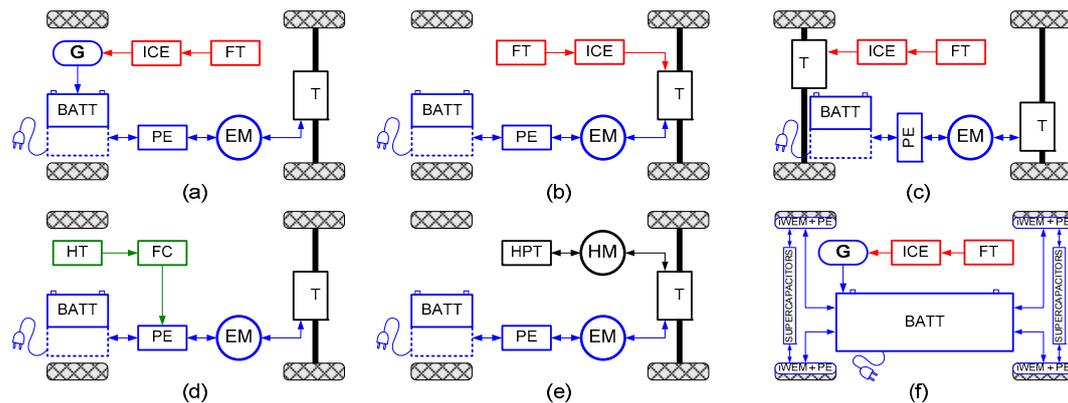
Figure 1. Sample configurations of hybrid drive systems: (**a**) serial hybrid drive, (**b**) parallel hybrid drive, (**c**) parallel hybrid drive, (**d**) serial hybrid drive with fuel cell, (**e**) parallel hybrid drive with hydraulic motor, (**f**) hybrid drive system with motors and converters mounted in a wheel; BATT—Battery Pack; EM—Electric Motor; HM—Hydraulic Motor; ICE—Internal Combustion Engine; FT—Fuel Tank; HT—Hydrogen Tank; HPT—High Pressure Tank, FC—Fuel Cell; G—Generator; PE—Power Electronics; iWEM—In Wheel Electric Motor; T—Transmission.

The ideal car should be emission-free, quiet, environmentally friendly, with a driving range of around 1000 km (620 miles) and inexpensive in daily operation. Most of these requirements could be met by various electric vehicle configurations (Figure 2), however obstacles are caused by the current energy storage devices.
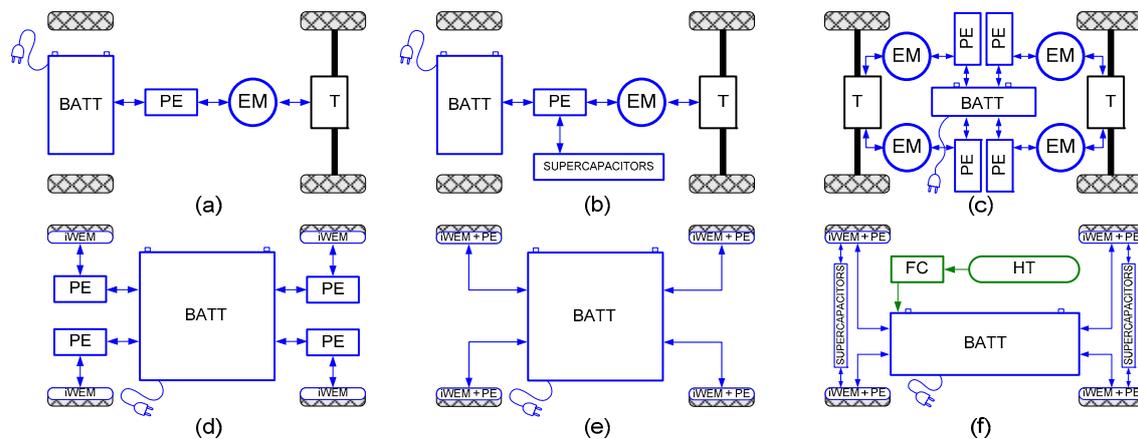

Figure 2. Sample configurations of xEV drive systems: (**a**) classic drive system, (**b**) drive system with supercapacitors, (**c**) drive system with four independently operating motors and converters mounted on the vehicle body, (**d**) drive system with independently operating engines mounted in wheels and converters mounted on the vehicle body, (**e**) drive system with independently operating motors and converters mounted in wheels, (**f**) drive system with independently operating motors and converters mounted in wheels, supercapacitors and fuel cell.

The list of shortcomings is long, and includes low energy density in comparison to liquid fuels, limits on charging/discharging current values (power density), limited power available from the public electrical distribution grid (available connection power, connection capacity to receive energy for bi-directional chargers mounted on the vehicle) [20,21], and finally, limited operating temperature. The solution could be to develop batteries with very high energy density of up to 1–1.5 kWh/kg, or employ a miniature nuclear reactors operating, for example, on a thorium-uranium cycle (Th-U) [22]. Unfortunately, neither technology is yet available and therefore alternative solutions are desired. The use of an additional source of electricity on the vehicle or attached trailer can be a solution to this issue. One of the first technologies that was commercially introduced to increase coverage and

reduce CO_2 emissions at the same time was the hybrid drive (HEV) technique, in serial or parallel configuration (Figure 1), combining the capabilities of the ICE and the electric motor. This concept assumed the placement of an additional source of energy on board the vehicle in addition to the battery pack.

At the end of the nineties, hybrid vehicles could be found in the offerings of automotive manufacturers. Currently, these designs are modified to increase the capacity of the battery pack with the possibility of simultaneous charging from the power grid (PHEV). With the development of hybrid vehicle technology (HEV, PHEV, FCEV), vehicles powered exclusively from the battery pack (BEV) were also developed. The tendencies of the governments that have recently been observed aim at elimination of the ICE from the propulsion systems. Following this line of reasoning, and knowing that according to statistics, more than 80% of drivers do not travel more than 65 km per day [23], it would be possible to completely remove the ICE from the hybrid vehicle and install an additional battery pack or supercapacitor bank in its place, or a hydrogen tank feeding a fuel cell [24]. Bearing in mind constraints in the form of proposals related to the phase out of conventional ICE propulsion units from vehicles, and the low range of BEV vehicles, it was suggested to attach a trailer with a generator set or other energy source [25] to the xEV vehicle (Figure 3). Such a solution called range extender (RE, REX), or alternatively range extending trailer-generator, long ranger, gen set trailer, etc., allows one to operate an electric vehicle over long distances, for example when traveling between cities. In built-up areas, however, it is always possible to detach the range extender range (REX) and use the battery pack installed in the vehicle. In the world literature, one can also find REs in which reduction of greenhouse gas (GHG) emissions caused by the ICE used to increase the range of an electric vehicle is accomplished by powering them with liquefied petroleum gas (LPG), liquified natural gas (LNG), hydrogen, alcohol or biofuels [26].
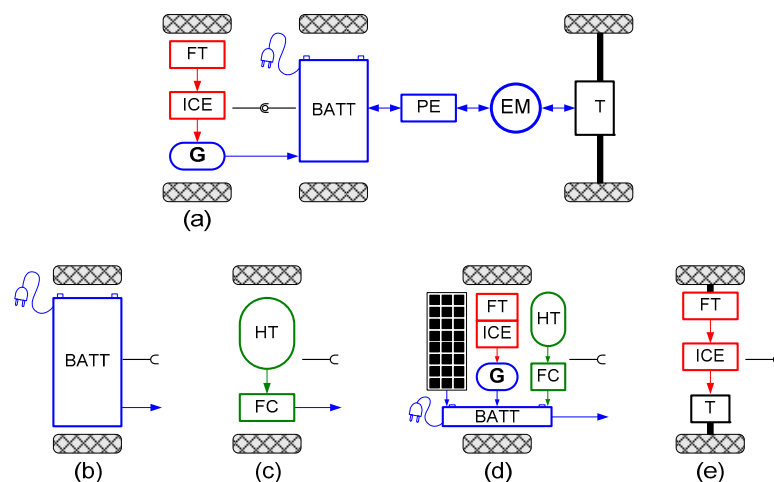

Figure 3. Exemplary structure of electrical drive system with range extender: (**a**) with an internal combustion generator; (**b**) with a package of electric batteries; (**c**) with a hydrogen cell; (**d**) hybrid system with photovoltaic panels, an internal combustion generator, a hydrogen cell and a packet of electric batteries; (**e**) system pushing a tow vehicle, with a combustion engine transmitting mechanical drive to the trailer's wheels. BATT—Battery Pack, EM—Electric Motor, HT—Hydrogen Tank, FT—Fuel Tank, FC—Fuel Cell, PE—Power Electronics, iWEM—In Wheel Electric Motor, T—Transmission, ICE—Internal Combustion Engine; G—Generator; PE—Power Electronics.

The generator sets of these types can be placed directly on the xEV vehicle or onto an attached trailer. One of the first actual designs using ICE-powered generators on a trailer was developed in 1992 by Gage from AC Propulsion (San Dimas, CA, USA) and Alan Cocconi (RXT) [27], the creator of the technology currently used by Tesla, Inc.(Palo Alto, CA, USA) In 2011 at the Geneva Auto Show,

the Swiss company Rinspeed (Zurich, Swiss) presented a conceptual solution named Dock + Go which were colloquially called "backpacks" for small city cars [28].

A similar solution was introduced by EP Tender (Poissy, France) in 2013. The developed REX is equipped with a petrol engine driving a 25 kW generator to allow an increase of range of approx. 600 km (375 miles) for an A and B segment electric car [29].

In 2017 BVB INNOVATE GmBH (Blackesville, Swiss) has presented a solution using a trailer with a package of batteries up to 85 kWh that can power up the EV. Batteries on the trailer can be charged at fast charging stations [30] and can also be used as emergency energy sources, (just like the 13.5 kWh Powerwall by Tesla). In this work, the author presents the results of research related to the application of a RE (placed upon a trailer) for an BEV. In order to reduce fuel consumption and cut down emissions of toxic gases, the technique of adding steam and oxyhydrogen gas (HHO) to the intake manifold of engine was applied.

2. Methods of GHG Reduction in ICEs

Regulations aim to reduce greenhouse gas (GHG) emissions, which mainly include carbon dioxide (CO_2), carbon monoxide (CO), nitrogen oxides (NO_x), sulfur oxides (SO_x) volatile non-methane organic compounds (NMVOC), hydrocarbons (HC), methane (CH_4), and particulate matter (PM) [31]. The simplest solution to reduce GHG emissions is to reduce the consumption of fuel used for propulsion of the vehicle. To achieve this goal, designers strive to reduce: vehicle weight, aerodynamic drag and rolling resistance. Research is also being carried out into the development of energy—efficient drive motors, shift control algorithms, or driving style of the vehicle driver. Another approach involves the use of various fuels or fuel additives, as well as substances and chemical compounds that reduce fuel consumption or reduce toxic emissions.

2.1. Steam Addition to the Intake Manifold of an ICE

One of the proposed techniques that have an impact on the reduction of pollutants emitted by the vehicle, is the method employing the addition of steam to the intake manifold [32], water injection into the intake manifold [33] or application of 32.5% urea solution, known by the commercial name AdBlue, injected automatically into exhaust manifold before the Selective Catalytic Reduction (SCR) catalyst located in the exhaust gas line. With the last of these AdBlue substances, there may be problems related to the decrease in effectiveness in the situation of system operation in extreme temperatures or too long storage of the fluid. When the air temperature drops, the urea crystals start to precipitate in the liquid. An increase in temperature above 30 °C (86 °F) causes a decrease in the efficiency of the system, as a result of which harmful nitrogen oxides NOx and particulate matter (PM) escape into the atmosphere [34]. These emissions can be reduced by installation of PM filters in the exhaust line. The presented technique of reduction of pollutants by an ICE assumes the supply of steam or water injection into its intake air manifold or combustion chamber. In the case of steam technology, the energy required to produce it, is taken from the exhaust of the engine and supplied to the tank in which water is stored (Figure 4). The amount of steam supplied to the intake manifold of the engine air can be dosed via a solenoid valve controlled by a PLC or a microcontroller.
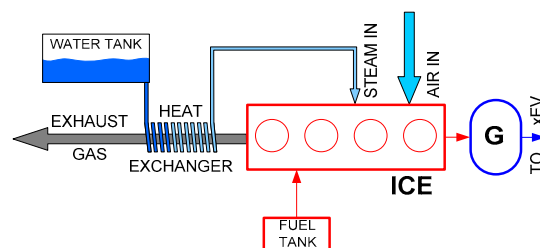

Figure 4. Block diagram of the system for steam delivery to the intake manifold of an internal combustion engine (ICE).

As part of the conducted tests, two engines of generator sets were tested: one running on petrol and another one on diesel fuel. The composition of exhaust gases was tested using the MRU 95/2D analyzer. Figure 5 shows the content of pollutants emitted by the engine of a generator in both the petrol and diesel versions.
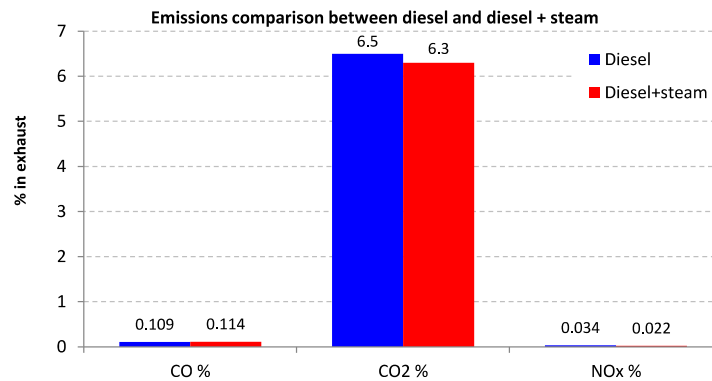

Figure 5. Content of pollutants in exhaust gases of a diesel generator set.

2.2. Oxy-Hydrogen (HHO) in Intake Manifold of ICE

Another way to reduce the emission of toxic substances from an ICE is the method using the addition of HHO gas into the air intake manifold of the ICE [35,36]. The electrical energy necessary to produce the HHO gas in the electrolysis process is supplied from an alternator driven by an ICE, to which the gas is then fed (Figure 6).
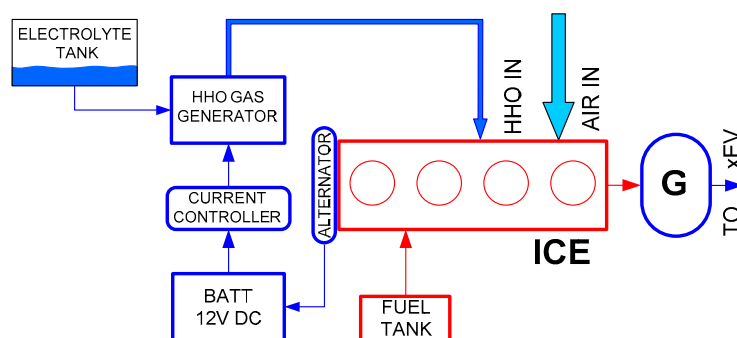

Figure 6. Block diagram of the system for oxyhydrogen (HHO) gas delivery to the intake manifold of an ICE together with diagram of the HHO gas generation system.

Sometimes there are solutions in which the hydrogen is supplied directly to the engine from the gas cylinder [37,38]. As part of the tests, the same two generators with petrol and diesel fuel types were tested. As in the case of steam addition measurements, the composition of exhaust gas content was tested using the MRU 95/2D analyzer. Figures 7 and 8 show the content of pollutants emitted by engines of petrol generator and diesel generator. Hybrid technologies are a form of substitute for the few disadvantages of BEV, which include relatively low range.
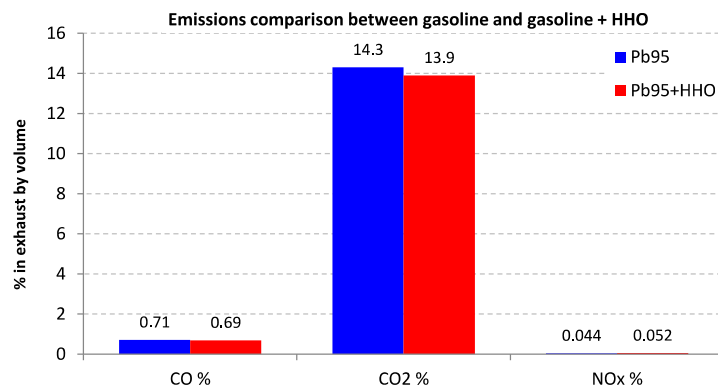
Figure 7. The amount of pollutants in the exhaust gases of a generator set with a gasoline engine.
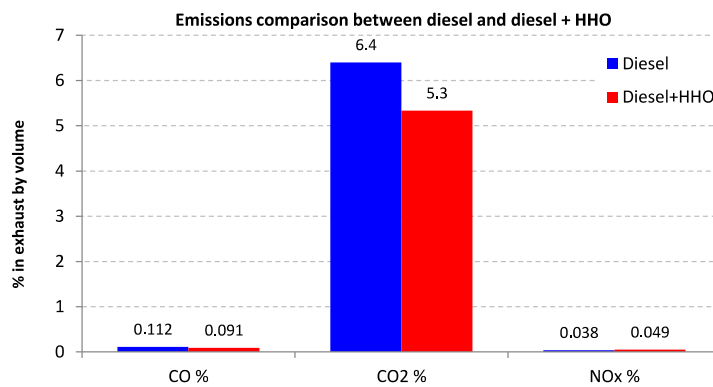
Figure 8. The amount of pollutants in the exhaust gases of a diesel generator set.

3. Modeling

In order to model a vehicle with a trailer in motion, the forces acting on both constructions during their movement should be taken into account (Figure 9).
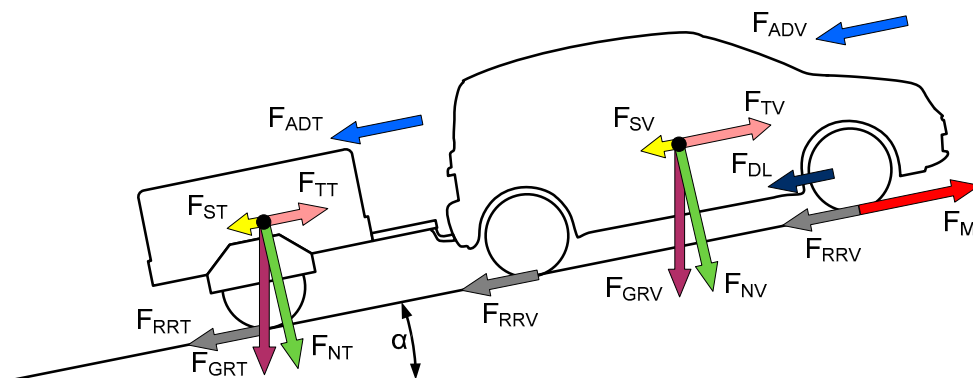
Figure 9. Forces acting on a moving vehicle with trailer.

The basic forces include those that are related to aerodynamic resistance, rolling resistance, sliding resistance, inertia resistance and resistances of the mechanisms in the propulsion system. For the vehicle to be able to move, the sum of forces associated with the resistances must be less than the force generated by the propulsion system. Table 1 gives a description of the symbols used and their meaning.

Table 1. Symbols and their meaning.

Symbol	Description	Unit	Symbol	Description	Unit
a	Acceleration of the vehicle	m/s^2	F_{TV}	Traction force acting on the vehicle	N
A_V	Frontal area of the vehicle	m^2	g	Standard gravity	m/s^2
A_T	Frontal area of the trailer	m^2	H_{sD}	Calorific value of diesel fuel	J/kg
C_{dV}	Vehicle drag coefficient	–	H_{sP}	Calorific value of petrol fuel	J/kg
C_{dT}	Trailer drag coefficient	–	I_B	Battery current	A
E_{REXD}	Electrical energy produced by diesel generator	J	I_M	Motor phase RMS current	A
E_{REXP}	Electrical energy produced by petrol generator	J	M_C	Torque at clutch at rated speed ω_{nC}	Nm
F_{AD}	Total aerodynamic drag force	N	M_{DS}	Torque at drive shafts at rated speed ω_{nDS}	Nm
F_{ADT}	Trailer aerodynamic drag force	N	M_F	Torque at gearbox output shaft at rated speed ω_{nF}	Nm
F_{ADV}	Vehicle aerodynamic drag force	N	M_M	Torque produced by the electric motor	Nm
F_{DL}	The force acting on the moving vehicle as a result of friction in the transmission system	N	m_{FD}	Mass of consumed diesel fuel	kg
F_{GRT}	Weight of the trailer	N	m_{FP}	Mass of consumed petrol fuel	kg
F_{GRV}	Weight of the vehicle	N	m_T	Trailer with range extender weight	kg
F_{IN}	Force inertia of the vehicle and trailer system	N	m_V	Vehicle weight	kg
F_M	Motive force created by the driven wheels	N	n_F	Final drive (differential gear) ratio	–
F_{NT}	Normal force of the trailer	N	n_G	Current transmission ratio	–
F_{NV}	Normal force of the vehicle	N	P_B	Battery power	W
F_R	Total resistance of the vehicle	N	P_{FD}	Chemical power flow of diesel fuel	W
F_{RR}	Total rolling resistance	N	P_{FP}	Chemical power flow of petrol fuel	W
F_{RRT}	Rolling resistance of trailer wheels	N	P_{REXD}	Diesel engine driven generator power	W
F_{RRV}	Rolling resistance of vehicle wheels	N	P_{REXP}	Petrol engine driven generator power	W
F_S	Total sliding force	N	P_I	Inverter power	W
F_{ST}	Sliding force acting on the trailer	N	P_M	Motor power	W
F_{SV}	Sliding force acting on the vehicle	N	R_V	Vehicle wheel radius	M
F_{TT}	Traction force acting on the trailer	N	R_T	Trailer radius of the trailer	M
U_B	Battery voltage	V	μ_{RRT}	Trailer wheels rolling resistance coefficient	–
v	Vehicle speed	m/s	ρ	Ambient air density	kg/m^3
α	Road inclination	deg.	ω_C	Clutch and input gearbox shaft rotation speed	rad/s
η_B	Battery efficiency	–	ω_{DS}	Average speed of wheel drive shafts	rad/s
η_{GD}	Diesel genset (engine + generator set) efficiency	–	ω_F	Gearbox output shaft rotation speed	rad/s
η_{GP}	Petrol genset (engine + generator set) efficiency	–	ω_{nC}	Nominal rotational speed of the clutch	rad/s
η_I	Inverter efficiency	–	ω_{nDS}	Nominal rotational speed of wheel drive shafts	rad/s
η_M	Motor efficiency	–	ω_{nF}	Nominal rotational speed of the gearbox output	rad/s
μ_{RRV}	Vehicle wheels rolling resistance coefficient	–			

The forces acting on the vehicle combination can be expressed on the basis of the relationship:

$$F_R = F_{AD} + F_{RR} + F_S + F_{DL} + F_{IN} \tag{1}$$

The aerodynamic drag forces for the vehicle combination were determined from the equations:

$$F_{AD} = F_{ADV} + F_{ADT} \tag{2}$$

$$F_{AD} = (C_{dV} \cdot A + C_{dT} \cdot A_T) \cdot \frac{\rho \cdot v^2}{2} \tag{3}$$

The rolling resistance forces for the vehicle combination were determined based on the dependence:

$$F_{RR} = F_{RRV} + F_{RRT} \tag{4}$$

$$F_{RR} = m_V \cdot g \cdot \frac{\mu_{RRV}}{R} \cdot \cos(\alpha) + m_T \cdot g \cdot \frac{\mu_{RRT}}{R_T} \cdot \cos(\alpha) \tag{5}$$

The sliding forces for the vehicle combination are based on:

$$F_S = F_{SV} + F_{ST} \tag{6}$$

$$F_S = (m_V + m_T) \cdot g \cdot \sin(\alpha) \tag{7}$$

The resistance forces of the transmission system related to the movement of the vehicle combination were determined basing on:

$$F_{DL} = R \cdot (M_C \cdot \frac{\omega_C}{\omega_{nC}} + M_F \cdot \frac{\omega_F}{\omega_{nF}} + M_{DS} \cdot \frac{\omega_{DS}}{\omega_{nDS}}) \tag{8}$$

wherein:

$$\omega_C = \omega_F \cdot n_G \tag{9}$$

$$\omega_F = \omega_{DS} \cdot n_F \tag{10}$$

$$F_{DL} = R \cdot \omega_{DS} \cdot \left(M_C \cdot \frac{n_G \cdot n_F}{\omega_{nC}} + M_F \cdot \frac{n_F}{\omega_{nF}} + M_{DS} \cdot \frac{1}{\omega_{nDS}} \right) \tag{11}$$

Inertia resistance forces related to the acceleration and braking of the vehicle combination were obtained based on:

$$F_{IN} = m_V \cdot a + m_T \cdot a = (m_V + m_T) \cdot a \tag{12}$$

The source of the driving force is the torque generated by the electric motor driving the wheels through: clutch, gearbox, differential and drive axles:

$$F_M = \frac{M_M \cdot n_G \cdot n_F}{R_V} \tag{13}$$

The driving power on the wheels is equal to the product of the linear speed v and the driving force F_M:

$$P_V = v \cdot F_M \tag{14}$$

Since the losses of the transmission are taken into account in the description of the F_{DL} force, it can be assumed that the propulsive power on the wheels is equal to the driving power generated by the vehicle's engine:

$$P_M = P_V \tag{15}$$

The power of the electric drive motor is equal to the power generated by the inverter minus the efficiency of the motor at a given operating point. The motor power is equal to the product of the engine torque and its rotational speed:

$$P_M(t) = P_I(t) \cdot \eta_M(I_M, \omega_C) = M_M(t) \cdot \omega_C(t) \tag{16}$$

The power generated by the inverter is equal to the power taken from the battery pack and generators decreased by the efficiency factor of the inverter:

$$P_I(t) = (P_B(t) + P_G(t)) \cdot \eta_I \tag{17}$$

The power drawn from the battery pack is equal to the product of the current flowing through the battery and its voltage reduced by the efficiency coefficient:

$$P_B(t) = U_B(t) \cdot I_B(t) \cdot \eta_B \tag{18}$$

The power generated by the generator sets is equal to the product corresponding to the power of the fuel consumed and the efficiency of the generating set:

$$P_{GP}(t) = P_{FP}(t) \cdot \eta_{GP} \tag{19}$$

$$P_{GD}(t) = P_{FD}(t) \cdot \eta_{GD} \tag{20}$$

By generating electricity, the RE consumes fuel-petrol or diesel. Depending on the type of fuel selected, the parameters of the efficiency of fuel-energy conversion and the calorific value of a kilogram of fuel are defined.

The chemical power flow for petrol and diesel fuel, P_{FP} and P_{FD}, respectively, is defined as the product of the weight of fuel burned over time of $m_{FD}'(t)$ and $m_{FP}'(t)$ respectively and the corresponding calorific value of fuel H_{sD} and H_{sP}.

The mass of fuel consumed and energy produced from it by RE is determined by the equation:

$$\begin{cases} E_{REXD}(t) = \int_0^t P_{REXD}(t) \cdot dt \\ E_{REXP}(t) = \int_0^t P_{REXP}(t) \cdot dt \\ m_{FD} = \int_0^t \frac{E_{REXD}(t)}{\eta_{GD} \cdot H_{sD}} \cdot dt \\ m_{FP} = \int_0^t \frac{E_{REXP}(t)}{\eta_{GP} \cdot H_{sP}} \cdot dt \\ P_{FD}(t) = m_{FD}'(t) \cdot H_{sD} \\ P_{FP}(t) = m_{FP}'(t) \cdot H_{sP} \end{cases} \tag{21}$$

The calorific value H for diesel fuel equals: H_{sD} = 38 MJ/kg, and for unleaded petrol equals: H_{sP} = 32 MJ/kg. Based on the mass of fuel consumed and the CO_2 emission factor for diesel fuel (EF_D) and petrol (EF_P), the mass of emitted carbon dioxide generated by the generating set (diesel—m_{CO2D}), petrol—m_{CO2P}) is calculated as well as the total mass of the emitted carbon dioxide (m_{CO2}).

$$\begin{cases} m_{CO2D} = m_{FD} \cdot EF_D \\ m_{CO2P} = m_{FP} \cdot EF_P \\ m_{CO2} = m_{CO2D} + m_{CO2P} \end{cases} \tag{22}$$

The modeling of the emission of other gases—carbon monoxide and nitrogen oxides, is based on the volume of emissions recorded during real road tests, measured using an exhaust gas analyzer.

The basis for calculating the CO and NO_x emissions of each generating set is the mass of carbon dioxide emitted multiplied by the mass CO/CO_2 emission factor named k_{Cx} and the mass NO_x/CO_2 emission factor named k_{Nx}. The k_{Cx} and k_{Nx} values take into account the effect of additions given to the intake manifold of the ICE of the generating sets. The index of x coefficients defines the type of fuel, D for diesel and P for gas, respectively.

The total mass of emitted m_{CO} is the sum of the masses of carbon monoxide emitted by the diesel generator set (m_{COD}) and the petrol generating set (m_{COP}):

$$\begin{cases} m_{COD} = m_{CO2D} \cdot k_{CD} \\ m_{COP} = m_{CO2P} \cdot k_{CP} \\ m_{CO} = m_{COD} + m_{COP} \end{cases} \tag{23}$$

3.1. Description of Test Vehicle Parameters

For research purposes, a mathematical model has been developed that describes the properties of a set of vehicles consisting of an electric Fiat Panda EV car with a trailer towed by it, equipped with diesel and petrol generators adapted for additives supply in the form of water steam and HHO (Figure 10).

Figure 10. Fiat Panda EV with RE on a trailer equipped with 5 kW gasoline and 6.5 kW diesel gensets.

The mathematical model was developed on the basis of measurement data recorded in real road conditions during the operation of a vehicle set of an electric car with a towed RE. The electric propulsion system of the vehicle consisted of a PMSM synchronous motor with a rated power of 50 kW powered by an IGBT inverter from a 19 kWh battery pack. The average energy consumption of a vehicle without a RE at an average speed of 50 kph (30 mph) was approximately 120 Wh/km (195 Wh/miles). The weight of the vehicle during the tests, including the driver, passengers and luggage was 1300 kg. The weight of the trailer with gensets and fuel was approximately 350 kg. The developed mathematical model of the vehicle assembly involves two configurations of generators. The first one consists of a 5 kW petrol generator and a 6.5 kW diesel generator, and the second one consisting of a single 20 kW diesel generator. The actual fuel consumption of the petrol unit was 2.34 dm^3/h, and for the diesel unit 1.28 dm^3/h. The fuel consumption for the 20 kW genset was 3.93 dm^3/h.

3.2. Vehicle Architecture and Description of the Model

The OpenModelica software package was used to model the influence of water steam and oxyhydrogen additives on the quality of exhaust gases emitted by gensets used to increase the range of vehicles with electric drive [39]. The developed mathematical model of the vehicle assembly (Figure 11) describes an electric car with a RE towed on a trailer.
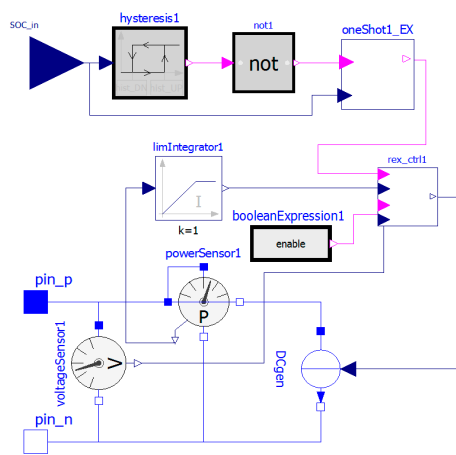
Figure 11. Implementation of the electric vehicle with RE in Modelica.

The car contains subsystems, such as: electric drive system (motor, inverter, battery pack), gearbox, torque transmission system. Additionally, model contains a block which represents resistance acting on the moving vehicle and a block tasked with specifying the route parameters like: speed profile and route elevation profile. In the resistance block, the forces acting during the movement of the vehicle combination—an electric car with a trailer RE are modeled. In the resistance block, there are modeled 3 of 4 resistance sources acting on the vehicle combination:

- aerodynamic resistance—common for the vehicle set,
- rolling resistance of the vehicle wheels, and rolling resistance of the trailer wheels,
- resistance related to the sliding force acting on a set of vehicles when the vehicle set travels on an inclined road section.

The fourth and last source of resistance, i.e., one that arises in the drive transmission system, is modeled in the transmission block.

The range extender block (Figure 12) models one generator set consisting of an ICE coupled with an electrical generator. The generating set is switched ON and OFF depending on the state of charge (SOC) of the traction battery. The generator set is switched ON and OFF after the SOC drops below/rises above the thresholds set by the operator. At the same time, the amount of fuel burned, depending on the load, type of fuel and additives: steam and/or HHO is calculated, along with the emitted amount of toxic gases: CO, CO_2, NO_x.

The developed model of the traction battery pack (Figure 13), mirrors the behavior of the actual battery pack in the vehicle along with the accompanying thermal phenomena (self-heating, increase of internal resistance with temperature drop) and the thermal conditioning system of the battery pack (cooling/heating battery pack).

Figure 12. Modeling of the range extender generator set in Modelica.

The battery pack is modeled using three main components: an adjustable voltage source block, a variable resistance block, and a heat capacity block. The adjustable voltage source block symbolizes the electromotive force (EMF) of the battery that changes with the state of charge (SOC) of the battery pack. The variable resistance block characterizes changes in the internal resistance of the cells of the battery pack, and is the place where the thermal losses emerge. The resistance change takes place in accordance with the temperature characteristic defined for the type of cells from which the battery pack is built. The heat capacity block represents the heat capacity of all cells in the battery pack. The battery pack block has the ability to configure parameters defining: number of single cells connected in parallel, number of cells connected in series, thermal capacity of a single cell in J/K, thermal conductivity between cells and the environment in W/K, initial temperature of the battery pack in degrees K and the initial state of charge (SOC). The last parameter contains a name of parameter record which characterizes the cells which the battery pack is built with. The record includes, among others, characteristics of EMF as a function of the cells state of charge, dependence of battery internal resistance as a function of cell temperature and single cell capacity in ampere-hours.
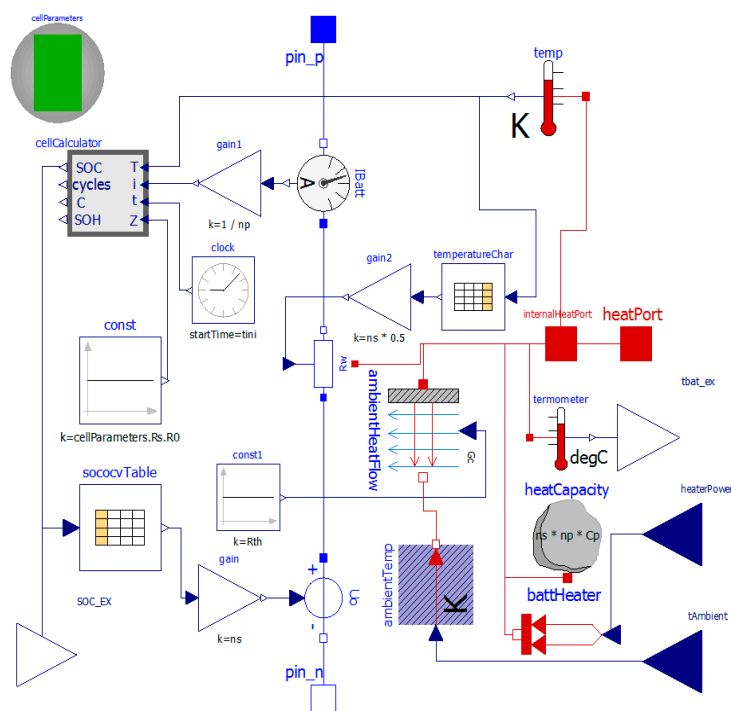

Figure 13. Modeling of the battery pack in Modelica.

In addition to the main elements mentioned above, the traction battery package model also includes auxiliary blocks that affect the operation of the battery model as a whole. The ammeter block, acts together with the cell calculator block, whose task is to monitor the currents flowing through the battery pack, to calculate the value of the actual state of charge of the battery pack. Another block is the heat flow block between the battery pack, the thermal conditioning system, and the surrounding ambient air.

The road parameter block is responsible for modeling the route parameters that the vehicle is travelling. Route details are stored in two text files. The first one contains the current value of the road slope and the elevation profile as a function of distance from the starting point. The second file describes the speed at which the vehicle is to drive on a given section of the route. For modeling purposes, two formats of vehicle speed description were developed. The first one describes the speed depending on time and is adapted to work with standard speed profiles used in fuel consumption tests on vehicles with conventional drive, carried out by US agencies (e.g., EPA Federal Test Procedure also known as FTP-75) and European (New European Driving Cycle—NEDC—and the Worldwide harmonized Light vehicles Test Procedure or WLTP). The second data format describes the target speed of the vehicle depending on the distance traveled.

The input signal for the road parameter block is information about the current distance from the starting point expressed in kilometers. On its basis, values related to the vehicle speed at a given moment, the current slope of the road in degrees and information about the parking brake activation or deactivation are calculated and transmitted to the transmission control block, which cooperates with the predictive reference model of vehicle position. The predictive reference model block, basing on information about the altitude profile of the route, has the task of controlling the vehicle speed by taking into account changes in the slope of the terrain so as to optimally use the kinetic energy of the vehicle during hill descents and subsequent ascents.

4. Simulations Results

The traction results in the Modelica package were made for a 609 km (380 miles) route between the cities of Gdynia and Cracow, which elevation profile shown on Figure 14 was obtained from the Google Earth service, and takes into account the route type and speed limits set on a given section of the route.
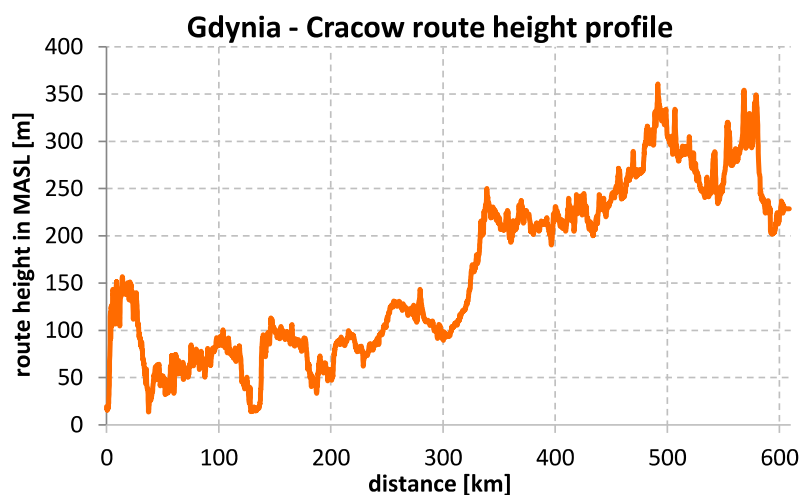

Figure 14. The elevation profile of the modeled route with length of 609 km (380 miles) between the cities of Gdynia and Cracow.

Thus, roads in built-up areas have a speed limit of 50 kph (30 mph), roads outside built-up areas have speed limits up to 70, 90, 100, 120 and 140 kph (45, 55, 60, 75 and 85 mph).

4.1. Emission of CO_2, CO, NO_x

The results of the research on pollutant emissions from combustion engines used in generators supplying the electric car are shown in Figures 15–21.

The lowest CO_2 emission level was obtained for the RE equipped with a 20 kW diesel generator with HHO gas supplied to the intake manifold of its engine, and the largest emission was obtained for the RE equipped with two generators: one 5 kW petrol and second 6.5 kW diesel, both without any additives (Figure 15).
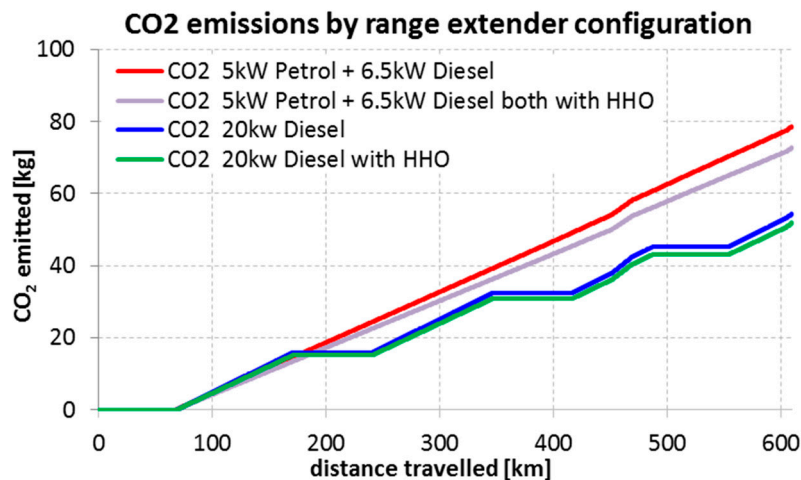

Figure 15. Comparison of CO_2 emissions by ICE of 20 kW diesel generator against 5 kW petrol and 6.5 kW diesel generators.

The CO_2 emissions for petrol and diesel generators with HHO gas were 4.6% lower than without addition of HHO, and for single 20kW diesel generator the CO_2 emissions with HHO were lower by 8% than without it. For the same route, an electric vehicle powered from a RE equipped with a 20 kW diesel generator would emit about 42% less CO_2 in relation to the RE powered by 5 kW petrol generator and 6.5 kW diesel generator, both HHO assisted. An increase in the speed of travel by 10 kph (6 mph) contributed to the increase in CO_2 emissions on the test section of 609 km (380 m) by about 6.5%. The amount of CO emitted for a 20 kW diesel generator was lower by 3.2% when HHO was injected into the intake manifold and 6% higher when water steam was fed, in relation to engine operating without any additives (Figure 16).
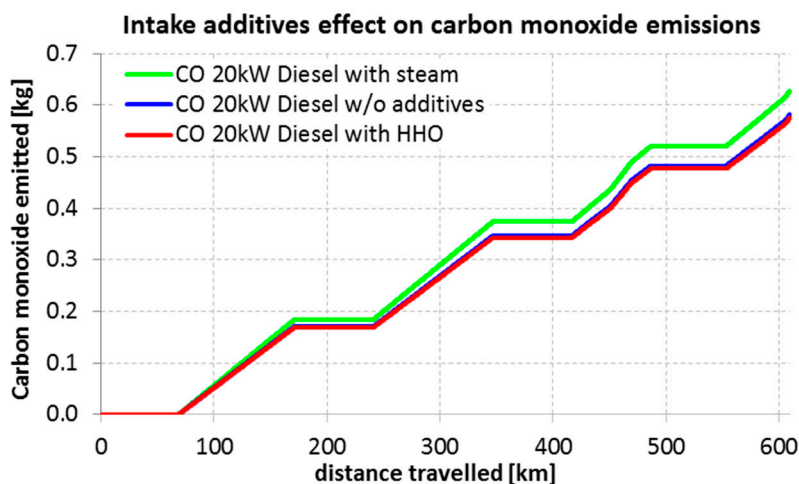

Figure 16. Comparison of CO emissions by the diesel engine of a 20 kW generator depending on the application of steam or HHO additives.

For a 20 kW diesel genset, about 48% lower NO_x emissions compared to normal emissions were reported when water steam was injected into the engine intake manifold and about 42% higher emissions were present when HHO was delivered (Figure 17).
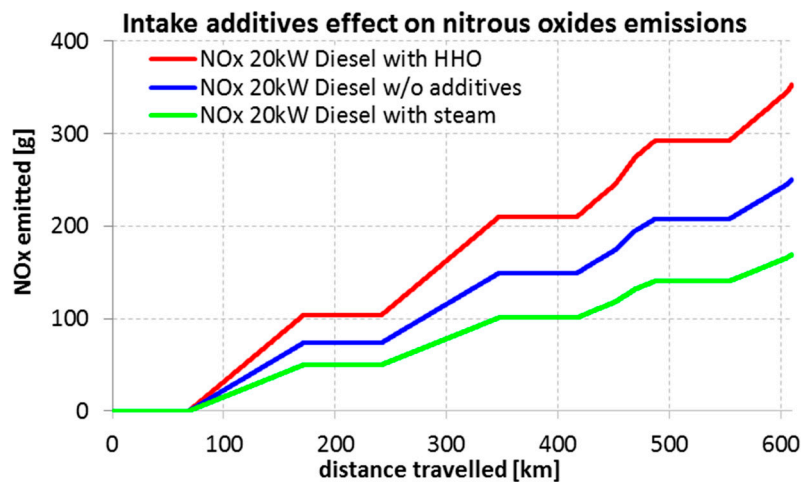
Figure 17. Comparison of NO_x emissions by the diesel engine of a 20 kW diesel generator set depending on the application of steam or HHO additives.

4.2. Energy Consumption

The addition of water steam or HHO gas to the intake manifolds of ICE, resulted in the change in the amount of fuel consumed by them. The lowest travel costs on the test route (the lowest fuel consumption) were obtained for the RE with a 20 kW diesel engine assisted by HHO (Figure 18). The use of HHO reduced the travel costs by approx. 5%.
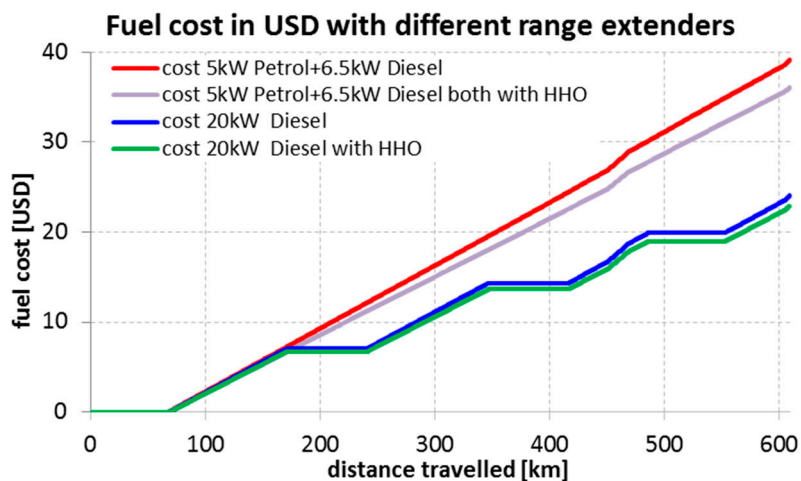
Figure 18. Comparison of travel costs for a test route of 609 km (380 m) for an electric vehicle powered by 20 kw diesel generator or 5 kW petrol and 6.5 kW diesel generators both with, and without HHO.

Vehicle travel costs using a RE equipped with a 5 kW petrol genset and 6.5 kW diesel genset fed with HHO were lower by 8.5% compared to the same setup without HHO. Travel costs with a RE equipped with a 20 kW diesel generator supplied with HHO were lower by approx. 60% compared to similarly assisted 5 kW petrol and 6.5 kW diesel generators. Such large differences in travel costs result mainly from higher efficiency of diesel engines (about 40%) compared to petrol engines (about 18%). During the research, the influence of the SOC_{ON-OFF} coefficient on the amount of fuel consumed was analyzed. The coefficient describes the level of charge of the battery pack, at which the generators are switched ON and turned OFF. The studies were carried out for SOC_{30-95}, SOC_{30-90}, SOC_{30-80}, SOC_{20-80},

and SOC_{20-90}. The obtained test results revealed that the value of the adopted SOC_{ON-OFF} coefficient affects the fuel consumption of power units powered by an electric vehicle, but for a strictly defined distance of the route.
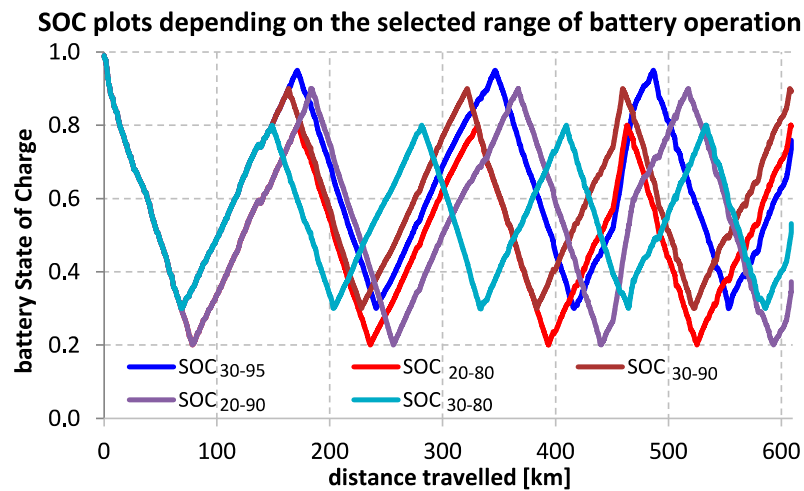
SOC plots depending on the selected range of battery operation

Figure 19. Block diagram of the system for steam delivery to the intake manifold of an ICE.

This dependence obviously translates into the amount of toxic substances emitted. By choosing the right value of the SOC_{ON-OFF} coefficient for a given distance, one can reduce the fuel consumption consumed by the gensets. For a 609 km (380 m) long route, the lowest fuel consumption was recorded for SOC_{20-90} and the highest for SOC_{30-90} (Figure 19).

At the same time, it should be borne in mind that for lithium batteries, narrowing the SOC_{ON-OFF} operating area or increasing the SOC_{ON} value (turning the generator before the battery discharges too deep) contributes to extending their service life (SOH) [40].

Figure 20 shows the SOC comparison for two different sets of generator sets installed on the RE. The SOC plot for a 20 kW diesel generator operating in the SOC_{30-95} range is shown in blue. From the presented plot it can be inferred that the power of the genset is a bit too high and there are periods in which the generator is turned OFF. The generator should not stop for extended periods of time which may cause excessive cooling of the engine and its inefficient operation. The SOC for 5 kW petrol and 6.5 kW diesel aggregates working in the first case for SOC_{30-95} and the second SOC_{80-95} are shown in red and brown.

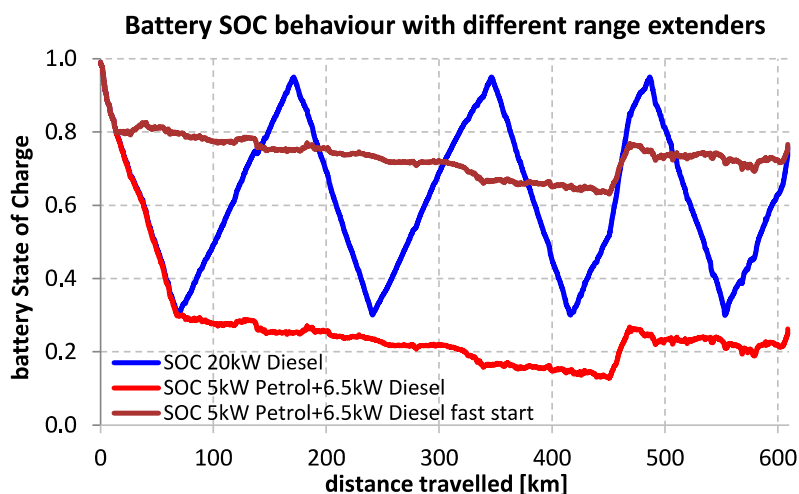**Battery SOC behaviour with different range extenders**

Figure 20. A comparison of electric vehicle battery SOC on a distance of 609 km (380 miles) for a 20 kW diesel genset as well as for 5 kW petrol and a 6.5 kW diesel gensets.

From the presented chart it can be seen that assuming too low level of SOC_{ON} (Figure 20, labeled "5 kW Petrol + 6.5 kW Diesel"), can cause the battery pack to become discharged too deeply at generators with low power which can cause vehicle immobilization due to the lack of electricity in the battery pack. Therefore, a better setting in a situation where generators do not have enough power to cover the whole vehicle's demanded energy is to set a higher level of SOC_{ON} (Figure 20, labeled "5 kW Petrol + 6.5 kW Diesel fast start").

Figure 21 shows the charge level of the battery pack for a 609 km (380 miles) distance traveled at a constant operating speed of 70 kph (45 mph) for one case and 80 kph (45 mph) for the other at SOC_{30-95}.
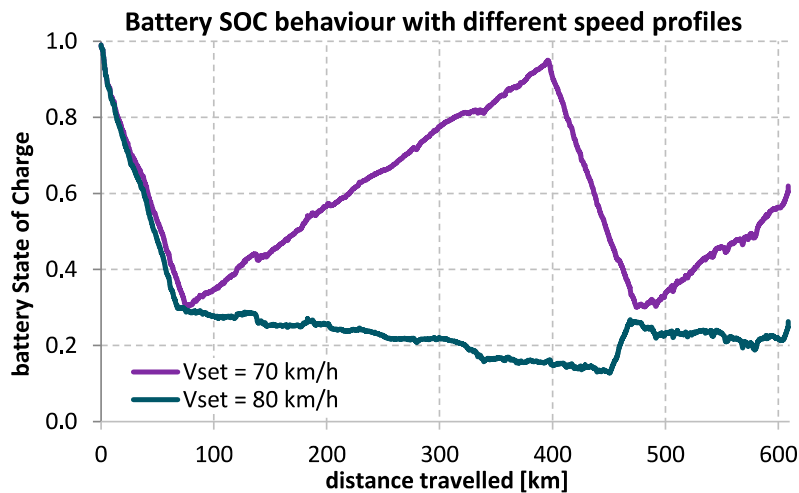

Figure 21. SOC comparison of battery pack assisted by from 5 kW petrol and 6.5 kW diesel generators for vehicle speeds of 70 kph (45 mph) and 80 kph (45 mph).

As shown in Figure 21, an increase in vehicle speed by 10 kph (6 mph) caused a significantly different course of battery charge status, which is obviously associated with spent fuel and the amount of pollutants emitted to the atmosphere. Bearing in mind the presented research results, it should be stated that the selection of a particular SOC_{ON-OFF} value should be subject to optimize taking into account a number of physical factors (ambient temperature, route height profile, route speed profile) as well as information that the vehicle user could provide (route length, level charge the battery pack after reaching the destination). Such a way of operation of RE contributes to both reducing the costs of operating an electric vehicle (as electricity produced in gensets is more expensive than electricity consumed from the power grid), and toxic gas emissions to the atmosphere by exploiting the possibility of covering the last section of the route without switching on generators.

5. Conclusions

On the basis of real traction tests of a set of vehicles consisting of an electric car and a trailer with generating sets, a mathematical model was developed in the Modelica environment, for which many research scenarios were carried out. The conducted simulation tests have shown that it is possible to reduce the emission of some toxic gases to the atmosphere produced by ICE of electrical generator sets when steam or HHO gas is fed into the intake air manifold (Figures 7 and 8).

For a gasoline engine assisted with the addition of HHO to the air intake manifold, a decrease of CO and CO_2 emissions by approx. 3% was noted, as well as an increase of NO_x content by around 15%. At the same time, the petrol engine supplied with HHO additives showed a 10% reduction in fuel consumption.

The diesel engine assisted by the addition of HHO to the air intake manifold showed a decrease in CO emissions by approx. 19%, a decrease in CO_2 emissions by approx. 17%, and an increase in NO_x

emissions by approx. 22%. Adding additives to the engine intake manifold in the form of HHO gas contributed to a 5% reduction in fuel consumption.

Diesel engine assisted by the addition of water steam to the air intake manifold, showed an increase in CO emission by approx. 4%, a decrease in CO_2 emissions by approx. 3%, and a decrease in NO_x emissions by approx. 35%. At the same time, when using water steam for a diesel generator, a slight increase in fuel consumption of 0.35% was observed.

The effect of water steam and HHO gas additives on the durability and service life of pistons, cylinders, valves, intake and exhaust systems was not analyzed in this research. Waste heat from gensets could be used in the future to heat the battery pack and vehicle cabin, if such need arises. The amount of gases emitted during the operation of an electric car with a RE is influenced by the assumed level of charge of the SOC_{ON-OFF} battery pack, for which the generator set is switched ON/OFF. The SOC_{ON-OFF} value should be set for the assumed distance to be traveled. Not without significance is also the impact of the travel speed of an electric vehicle equipped with towed RE.

The conducted research has demonstrated the benefits of development and application of trailer mounted range extenders with modules optimizing the fuel consumption for support of electric drive systems.

References

1. Zhang, Z.; Zhang, R.; Cescatti, A.; Wohlfahrt, G.; Buchmann, N.; Zhu, J.; Chen, G.; Moyano, F.; Pumpanen, J.; Hirano, T.; et al. Effect of climate warming on the annual terrestrial net ecosystem CO_2 exchange globally in the boreal and temperate regions. *Sci. Rep.* **2017**, *7*. [CrossRef] [PubMed]
2. Greg, A. Cars and CO_2. Available online: www.transportenvironment.org/what-we-do/cars-and-co$_2$ (accessed on 24 July 2018).
3. Group, S. World's First Electric Road Opens in Sweden—Scania Group. Available online: https://www.scania.com/group/en/worlds-first-electric-road-opens-in-sweden/ (accessed on 24 July 2018).
4. Highway Agency. Preparing the Strategic Road Network for Electric Vehicles. A Research Programme GOV.UK 2014. Available online: http://assets.highways.gov.uk (accessed on 24 July 2018).
5. Un-Noor, F.; Padmanaban, S.; Mihet-Popa, L.; Mollah, M.; Hossain, E. A Comprehensive Study of Key Electric Vehicle (EV) Components, Technologies, Challenges, Impacts, and Future Direction of Development. *Energies* **2017**, *10*, 1217. [CrossRef]
6. Zeng, X.; Cui, H.; Song, D.; Yang, N.; Liu, T.; Chen, H.; Wang, Y.; Lei, Y. Jerk Analysis of a Power-Split Hybrid Electric Vehicle Based on a Data-Driven Vehicle Dynamics Model. *Energies* **2018**, *11*, 1537. [CrossRef]
7. Li, S.; Hu, M.; Gong, C.; Zhan, S.; Qin, D. Energy Management Strategy for Hybrid Electric Vehicle Based on Driving Condition Identification Using KGA-Means. *Energies* **2018**, *11*, 1531. [CrossRef]
8. Jankowski, P.; Mindykowski, J. Measurement of quantities characterizing the properties of an inductive dynamic drive. *Prz. Elektrotechniczn.* **2012**, *88*, 78–82.
9. Jankowski, P.; Wołoszyn, M. Suitability study of hybrid model of electrodynamic actuator. *Int. J. Appl. Electromagn.* **2014**, 649–657. [CrossRef]
10. May, H.; Palka, R.; Paplicki, P.; Szkolny, S.; Wardach, M. Comparative research of different structures of a permanent-magnet excited synchronous machine for electric vehicles. *Prz. Elektrotechniczn.* **2012**, *88*, 53–55.
11. Solouk, A.; Tripp, J.; Shakiba-Herfeh, M.; Shahbakhti, M. Fuel consumption assessment of a multi-mode low temperature combustion engine as range extender for an electric vehicle. *Energy Convers. Manag.* **2017**, *148*, 1478–1496. [CrossRef]
12. Muratori, M.; Bush, B.; Hunter, C.; Melaina, M. Modeling Hydrogen Refueling Infrastructure to Support Passenger Vehicles. *Energies* **2018**, *11*, 1171. [CrossRef]

13. Kere, L.; Kelouwani, S.; Agbossou, K.; Dube, Y. Improving efficiency through adaptive internal model control of hydrogen-based genset used as a range extender for electric vehicle. *IEEE Trans. Veh. Technol.* **2017**, 4716–4726. [CrossRef]

14. Passalacqua, M.; Lanzarotto, D.; Repetto, M.; Marchesoni, M. Advantages of Using Supercapacitors and Silicon Carbide on Hybrid Vehicle Series Architecture. *Energies* **2017**, *10*, 920. [CrossRef]

15. Zhao, K.; Liang, Z.; Huang, Y.; Wang, H.; Khajepour, A.; Zhen, Y. Research on a Novel Hydraulic/Electric Synergy Bus. *Energies* **2018**, *11*, 34. [CrossRef]

16. Zhang, R.; Xia, B.; Li, B.; Cao, L.; Lai, Y.; Zheng, W.; Wang, H.; Wang, W. State of the Art of Lithium-Ion Battery SOC Estimation for Electrical Vehicles. *Energies* **2018**, *11*, 1820. [CrossRef]

17. Rangaraju, S.; de Vroey, L.; Messagie, M.; Mertens, J.; van Mierlo, J. Impacts of electricity mix, charging profile, and driving behavior on the emissions performance of battery electric vehicles: A Belgian case study. *Appl. Energy* **2015**, *148*, 496–505. [CrossRef]

18. Vidhi, R.; Shrivastava, P. A Review of Electric Vehicle Lifecycle Emissions and Policy Recommendations to Increase EV Penetration in India. *Energies* **2018**, *11*, 483. [CrossRef]

19. Huo, H.; Cai, H.; Zhang, Q.; Liu, F.; He, K. Life-cycle assessment of greenhouse gas and air emissions of electric vehicles: A comparison between China and the U.S. *Atmos. Environ.* **2015**, *108*, 107–116. [CrossRef]

20. Masnicki, R.; Mindykowski, J. Coordination of operations in registration channel of data from electrical power system. *Measurement* **2017**, *99*, 68–77. [CrossRef]

21. Li, G.; Qian, B.; Shi, D.; Duan, X. Unit commitment problem of power system with plug-in electric vehicles. *Prz. Elektrotechniczn.* **2012**, *88*, 297–302.

22. Frybort, J. Equilibrium thorium fuel loading in VVER-1000 reactor. In Proceedings of the 2014 15th International Scientific Conference on Electric Power Engineering (EPE), Hotel Santon, Brno, Czech Republic, 12–14 May 2014; Drápela, J., Ed.; IEEE: Piscataway, NJ, USA, 2014; pp. 693–697.

23. European Commission; Alberto, D.; Panagiota, D.; Christian, T.; Alessio, S.; Dimitrios, G.; Ioannis, D. *JRC Science and Policy Report. Individual Mobility: From Conventional to Electric Cars*; Joint Publications Office of the European Union: Brussels, Belgium, 2015.

24. Grijalva, E.; López Martínez, J.; Flores, M.; del Pozo, V. Design and Simulation of a Powertrain System for a Fuel Cell Extended Range Electric Golf Car. *Energies* **2018**, *11*, 1766. [CrossRef]

25. Łebkowski, A.; Kopeć, Z. Mobile set for electric vehicle, has separate unit provided with intelligent power inverter, and intelligent power inverter controlling energy flow through power connector, where energy is stored in batteries. Patent PL388354-A1, 22 June 2009.

26. Raza, M.; Chen, L.; Leach, F.; Ding, S. A Review of Particulate Number (PN) Emissions from Gasoline Direct Injection (GDI) Engines and Their Control Techniques. *Energies* **2018**, *11*, 1417. [CrossRef]

27. The Beata Electric Motor Garrage Collection. ACP AC Propulsion LongRanger, Series Range Extending Trailer, Alan Cocconi, RXT-G, Hybrid Trailer, EV Range Extender, GenSet. Available online: http://www.tzev.com/1992_1995_2001_acp_rxt-g_.html (accessed on 26 July 2018).

28. Rinspeed AG. Rinspeed—Creative Think Tank for the Automotive Industry. Where the Future is Reality—Today. Available online: https://www.rinspeed.eu/en/Visionen (accessed on 26 July 2018).

29. EP Tender. Range Extending Service for Electric Vehicles. Available online: http://www.eptender.com/ (accessed on 24 July 2018).

30. Nomadic Power. Mobile Battery. Available online: https://bvb-innovate.com/mobilebattery/ (accessed on 24 July 2018).

31. Grammelis, P. *Energy, Transportation and Global Warming*, 1st ed.; Springer International Publishing: Cham, Switzerland, 2016.

32. Zhu, S.; Liu, S.; Qu, S.; Deng, K. Thermodynamic and experimental researches on matching strategies of the pre-turbine steam injection and the Miller cycle applied on a turbocharged diesel engine. *Energy* **2017**, *140*, 488–505. [CrossRef]

33. Mingrui, W.; Thanh Sa, N.; Turkson, R.F.; Jinping, L.; Guanlun, G. Water injection for higher engine performance and lower emissions. *J. Energy Inst.* **2017**, *90*, 285–299. [CrossRef]

34. Carley, J. Storing and Handling AdBlue Correctly: What Farmers Need to Know. Available online: https://www.fginsight.com/news/news/storing-and-handling-adblue-correctly-what-farmers-need-to-know-66270 (accessed on 26 August 2018).

35. EL-Kassaby, M.M.; Eldrainy, Y.A.; Khidr, M.E.; Khidr, K.I. Effect of hydroxy (HHO) gas addition on gasoline engine performance and emissions. *Alex. Eng. J.* **2016**, *55*, 243–251. [CrossRef]

36. Goldman, J.; King, D.; Meyer, R.; Petty, C.; Winslett, B.L.; Lee, J. Water vapor management and control methodology system for single and multiple hydrogen fuel cells used for combustion augmentation in internal combustion engines and method. Patent US20150040843, 8 August 2014.

37. Takagi, Y.; Mori, H.; Mihara, Y.; Kawahara, N.; Tomita, E. Improvement of thermal efficiency and reduction of NOx emissions by burning a controlled jet plume in high-pressure direct-injection hydrogen engines. *Int. J. Hydrogen Energy* **2017**, *42*, 26114–26122. [CrossRef]

38. Czech, P. Diagnosing a Car Engine Fuel Injectors' Damage. In Proceedings of the 13th International Conference on Transport Systems Telematics, TST 2013 Katowice, Ustroń, Poland, 23–26 October 2013; Springer: Berlin/Heidelberg Germany, 2013.

39. Open Source Modelica Consortium. OpenModelica. Available online: https://www.openmodelica.org/ (accessed on 26 July 2018).

40. Semanjski, I.; Gautama, S. Forecasting the State of Health of Electric Vehicle Batteries to Evaluate the Viability of Car Sharing Practices. *Energies* **2016**, *9*, 1025. [CrossRef]